ZIBELINE INTERNATIONAL™ PUBLISHING

Acta Scientifica Malaysia (ASM)

DOI: http://doi.org/10.26480/asm.02.2024.61.73

ISSN: 2521-5051 (Print)
ISSN: 2521-506X (Online)
CODEN: ASMCCQ

RESEARCH ARTICLE

EVALUATION OF THE ANTI-LEISHMANIAL POTENTIAL OF SOME PROMINENT LEAD COMPOUNDS AGAINST PYRIDOXAL KINASE IN COMPLEX WITH ADENOSINE DIPHOSPHATE AND PYRIDOXINE: A COMPARATIVE STUDY

Fabian Audu Ugbe[a*], Abdullahi Muhammad Ayuba[b], Emmanuel Israel Edache[c], Anne Jibrin[d], Oluwagbemiga Tayo Amusan[e]

[a] Department of Chemistry, University of Abuja, Abuja, Nigeria.
[b] Department of Pure and Industrial Chemistry, Bayero University Kano, Nigeria.
[c] Department of Pure and Applied Chemistry, University of Maiduguri, Maiduguri, Nigeria.
[d] Department of Chemistry, Air Force Institute of Technology, Kaduna, Nigeria.
[e] Department of Chemical Sciences, Ojaja University, Ilorin, Nigeria.
****Corresponding address Email: ugbefabianaudu@gmail.com***

ARTICLE DETAILS

Article History:

Received 23 July 2024
Revised 18 August 2024
Accepted 18 September 2024
Available online 02 October 2024

ABSTRACT

More than twelve million individuals globally suffer from leishmaniasis, and an additional billion people are at risk in leishmaniasis prevalent areas. This work was motivated by the need to create drugs with high efficacies against leishmaniasis and to overcome the shortcomings of current anti-leishmanial treatments. In this study, a molecular docking investigation was performed to assess the Pyridoxal kinase (PDB ID - 6K91) protein targeting ability of five lead molecules, one each of maleimide, arylimidamide-azole hybrid, arylbenzimidazole, diarylidene cyclohexanone, and organoselenium. The various compounds were further subjected to molecular dynamics (MD) simulation, generalized Born and surface area continuum solvation (MM/GBSA) calculation, drug-likeness assessment, and evaluation of ADMET properties. The overall average binding affinity of the molecules to 6K91 follows the order: B (-10.7 kcal/mol) > C (-10.5) > D (-9.1) > E (-8.7) > SD (-8.1) > A (-7.8 kcal/mol). The MD simulation results indicate these compounds' favourability and stability in binding to the target in the order; B > SD > C > E > D > A, while their estimated binding free energies in kcal/mol are in the order: B_6K91 (-88.2216) > D_6K91 (-57.4219) > SD_6K91 (-56.7839) > E_6K91 (-51.2518) > C_6K91 (-25.9665) > A_6K91 (unfavorable). The various compounds passed Lipinski's test and were said to be orally bioavailable, having also good ADMET properties that compare quite well to Pentamidine (standard drug). Conclusively, B (arylimidamide-azole hybrid) demonstrated the best anti-leishmanial attributes, and therefore, could be developed as a potential drug candidate for leishmaniasis.

KEYWORDS

Leishmaniasis, Pyridoxal kinase, Molecular docking, Drug-likeness, ADMET, Molecular dynamics

1. INTRODUCTION

According to a study, leishmaniasis is a dangerous infection that can range in severity from minor skin lesions to deadly visceral forms (Eldehna et al., 2019). It is caused by many species of *Leishmania*. Humans contract leishmaniasis when bitten by female Phlebotomine sandflies, which are found in 97 countries, mostly in tropical regions (Stevanovic et al., 2019; Ugbe et al., 2022a). According to other study, leishmaniasis frequently presents as visceral leishmaniasis (VL), mucocutaneous leishmaniasis (MCL), and cutaneous leishmaniasis (CL) (Stevanovic et al., 2019).

In regions where leishmaniasis is endemic, more than a billion individuals are susceptible to infection (Bekhit et al., 2022; Ugbe et al., 2022b). Leishmaniasis can only be treated with a limited number of medications, including miltefosine, pentamidine, amphotericin B, pentostam, and pacmomycin (Ashok et al., 2018; Ugbe et al., 2023a). These treatments have drawbacks, such as high costs, poor efficacy, and side effects (Fan et al., 2018). Nephrotoxicity, hypokalemia, myocarditis, and fever have all been linked to amphotericin B (Ghorbani et al., 2017; Ugbe et al., 2023b). Pentamidine's problem is that it can cause insulin-dependent diabetes, whereas paromomycin can cause ototoxicity and nephrotoxicity (Ugbe et al., 2023b). Furthermore, the organisms responsible for the problem consistently resist various treatments (Fan et al., 2018). Thus, it is imperative to find and create novel medications to overcome the shortcomings of current therapies.

Some classes of organic compounds, including maleimide, arylimidamide-azole hybrid, arylbenzimidazole, diarylidene cyclohexanone, and organoselenium, were previously investigated for their potential as anti-leishmanial agents. Maleimides have demonstrated strong enzyme inhibitory activity and have been described as antibacterial agents (Fan et al., 2018; Abdelhameed et al., 2021; Keurulainen et al., 2015; Din et al., 2018; Al-Tamimi et al., 2019; López et al., 2005; Slavica et al., 2007; Chen et al., 2015; Li et al., 2012; Shen et al., 2013). Furthermore, maleimides had previously been reported to have anti-anxiety, anti-inflammatory, and anti-cancer properties (Jerzy, 2003; Quintão et al., 2010; Khan et al., 2004). Additionally, compounds classified as arylimidamide-azole incorporate both an azole and an arylimidamide moiety in their structures.

These compounds have been shown to improve the pharmacokinetics and/or pharmacodynamics of these classes of molecules in vivo, as well as have the advantage of interacting with the targets of both classes of compounds (Abdelhameed et al., 2021). Furthermore, a number of medications that are used to treat different medical diseases contain the

Quick Response Code	Access this article online	
	Website: www.actascientificamalaysia.com	**DOI:** 10.26480/asm.02.2024.61.73

Cite The Article: Fabian Audu Ugbe, Abdullahi Muhammad Ayuba, Emmanuel Israel Edache, Anne Jibrin, Oluwagbemiga Tayo Amusan (2024). Evaluation of The Anti-Leishmanial Potential of Some Prominent Lead Compounds Against Pyridoxal Kinase in Complex with Adenosine Diphosphate and Pyridoxine: A Comparative Study. *Acta Scientifica Malaysia, 8(2): 61-73.*

benzimidazole structure (Keurulainen et al., 2015). Also, leishmanial inhibitory studies have been conducted on compounds derived from benzimidazole (Patle et al., 2013; Shaukat et al., 2013; Torres-Gómez et al., 2008). Additionally, a variety of actions, including anti-tumor, anti-tubercular, anti-inflammatory, and anti-oxidant properties, have been identified for Bis-(arylmethylidine)-cycloalkanones (Din et al., 2018).

It has also been shown that the two aromatic moieties in bis-aryl-α, β unsaturated ketones are significant for the possibility of ligand binding to a particular target protein (Chandru et al., 2007). The synthesis of various biologically active molecules and significant medicinal products has made organoselenium chemistry an exceptional field in recent years. Research on the creation and synthesis of organoselenium compounds with enhanced biological activity is still ongoing (Akhoon et al., 2015). A wide range of biological activities have been reported for organoselenium compounds, including anti-inflammatory, antioxidant, neuroprotective anti-cancer and anti-diabetic (Bjørklund et al., 2022; Mamgain et al., 2023; Dominiak et al., 2016; Landgraf et al., 2020; Gandin et al., 2018; Radomska et al., 2021; Nishiguchi et al., 2017).

A variety of intriguing therapeutic protein targets, including ribokinase, ribosome, Pyridoxal kinase (PdxK), UMP synthase, O-acetylserine sulfhydrylase (OASS), and others are identified among the different Leishmania species (Are et al., 2020; Gatreddi et al., 2019; Soufari et al., 2020) (French et al., 2011)Raj et al., 2012). PdxK is an intriguing target for anti-leishmanial medications. According to Are et al., it aids in accelerating the phosphorylation of the pyridoxal's 5´ hydroxyl group to produce pyridoxal-5´-phosphate, an active form of vitamin B6 in the body (Are et al., 2020). PdxK contributes significantly to the proliferation of parasites and intensifies host infection (Kumar et al., 2018). Prior research has indicated that two well-known anti-malaria medications, primaquine and chloroquine, inhibit PdxK (Ugbe et al., 2023a). Thus, PdxK continues to be a viable target for new leishmania inhibitors, a case which informed its selection as the target protein in our study.

The use of computational approaches to drug discovery (CADD) has made it possible to expedite the drug discovery process by allowing for the rapid screening and synthesis of vast libraries of compounds (Ou-Yang et al., 2012). Low efficacy and high failure rates in drug discovery have been greatly lessened since the advent of CADD (Pathak et al., 2020). Molecular docking, binding free energy analysis, molecular dynamics (MD) simulation, pharmacokinetics analysis, and quantitative structure-activity relationships (QSAR) are a few frequently used CADD techniques (Edache et al., 2023a; Ugbe et al., 2023c; Lawal et al., 2021; Adeniji et al., 2020). Understanding QSAR facilitates the correlation between a compound's observed activities and its different molecular structures (Edache et al., 2023b). Using a legitimate docking tool, molecular docking simulation is a computer-aided screening technique that examines ligand binding in the active regions of protein targets (Edache et al., 2023b).

The scoring functions used by the docking algorithms are usually not well correlated with the experimental data; they are intended for quick assessment of the binding affinities for various postures produced by the searching algorithm (Sahakyan, 2021). Fortunately, more complex techniques exist for evaluating binding affinities, such as thermodynamic integration (TI), free energy perturbation (FEP), generalized Born and surface area continuum solvation (MM/GBSA), and molecular mechanics energies combined with the Poisson–Boltzmann (MM/PBSA) (Straatsma and Berendsen, 1988; Jorgensen and Thomas, 2008; Massova and Kollman, 2008). Since the MM/GBSA and MM/PBSA free energy calculation methods are more dependable than scoring functions and faster than FEP or TI, they are a good option (Sahakyan, 2021). To investigate the stiffness and stability of the protein-ligand interactions during a trajectory, MD simulation is required (Ugbe et al., 2023c).

As a result, a key strategy for researching protein-ligand interactions and drug development is the combination of docking, free energy computation, and MD modeling. Conversely, pharmacokinetics analysis plays a crucial role in pre-clinical research on novel therapeutic molecules to determine their effects on living organisms upon administration (Abdullahi et al., 2022). Absorption, distribution, metabolism, excretion, and toxicity (ADMET) are significant pharmacokinetic features typically ascertained during pre-clinical testing (Lawal et al., 2021; Ibrahim et al., 2021). To forecast a drug's probability of being orally accessible, physicochemical characteristics are required, including molecular weight, lipophilicity index, hydrogen bond donors, and hydrogen bond acceptors, among others (Lipinski et al., 2012).

A report on the *in-silico* exploitation of these five classes of anti-leishmanial chemical libraries to find novel pharmacological entities with significant anti-leishmanial properties can be found in the literature. To profile these compounds as potential anti-leishmanial drug candidates, this study focused on comparative molecular docking, MD simulation, drug-likeness assessment, and evaluation of ADMET properties.

2. Materials and Methods

2.1 Acquisition of Compounds

Five (5) anti-leishmanial compounds, one for each of maleimides, arylimidamide-azole hybrid, arylbenzimidazole, diarylidene cyclohexanone, and organoselenium were retrieved from the literature (Ugbe et al., 2022a; Ugbe et al., 2022b; Ugbe et al., 2023a; Ugbe et al., 2023b; Ugbe et al., 2023c). From the respective computational evaluation of these compounds' classes, the five compounds were been identified as lead molecules. The molecular structures of the retrieved lead molecules and the chosen standard drug are shown in Figure (1).

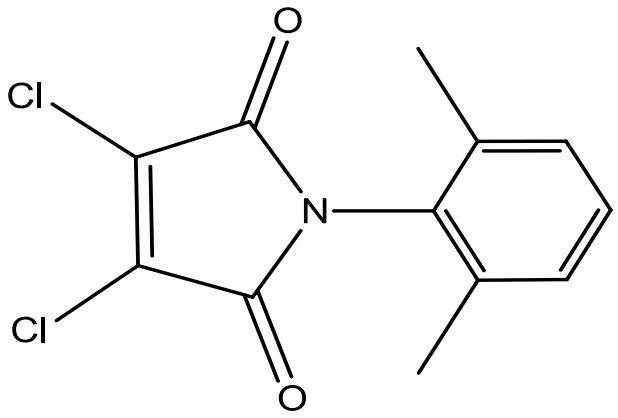

IUPAC name: 3, 4-dichloro-1-(2,6-dimethylphenyl)-1H-pyrrole-2,5-dione

Class of compound: Maleimide

Identification code: A

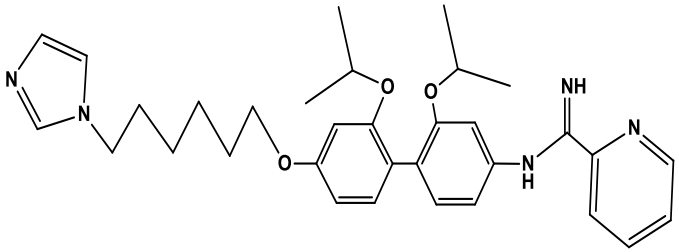

IUPAC name: N-(4'-((6-(1H-imidazol-1-yl)hexyl)oxy)-2,2'-diisopropoxy-[1,1'-biphenyl]-4 yl)picolinimidamide

Class of compound: Arylimidamide-azole hybrid

Identification code: B

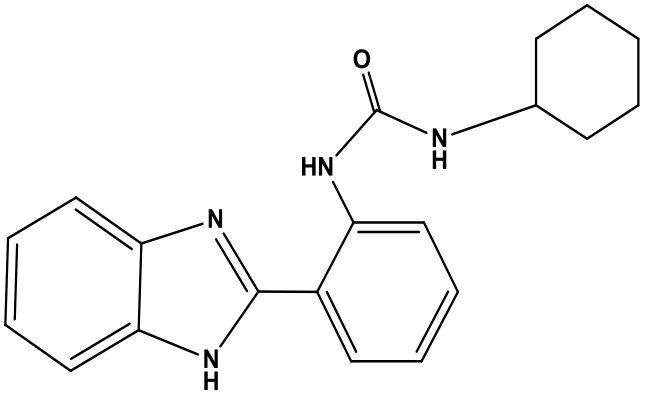

IUPAC name: 1-(2-(1H-benzo[d]imidazole-2-yl)phenyl)-3 cyclohexylurea

Class of compound: Arylbenzimidazole

Identification code: C

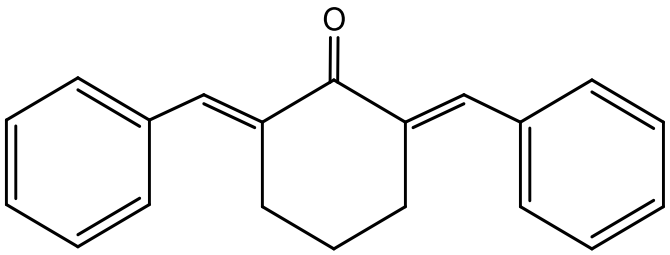

IUPAC name: (2E,6E)-2,6-dibenzylidenecyclohexanone

Class of compound: Diarylidene cyclohexanone

Identification code: D

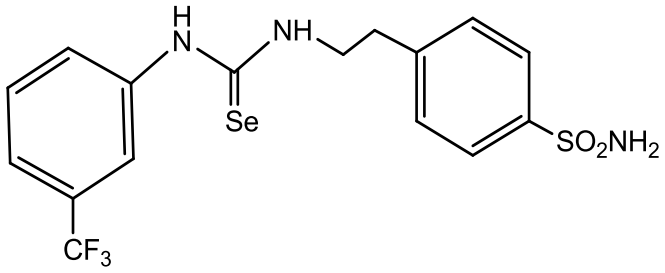

IUPAC name: 4-(2-(3-(
(trifluoromethyl)phenyl)selenoureido)ethyl)benzenesulfonamide

Class of compound: Organoselenium

Identification code: E

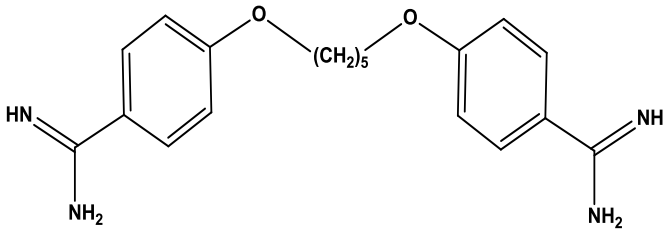

IUPAC name: 4,4'-(pentane-1,5-diylbis(oxy))dibenzimidamide

Class of compound: Diamidine

Common name: Pentamidine

Identification code: SD

Figure 1: Molecular structures of retrieved lead molecules and standard drug pentamidine

2.2 Geometry Optimization

ChemDraw Ultra software v12.0.2 was utilized to derive the 2-dimensional (2D) structures of the different compounds and the standard drug (SD), pentamidine (Ugbe et al., 2021; Ugbe et al., 2023c). Geometry optimization was done on the Spartan 14 v1.1.4 graphical user interface to find the least possible energy conformers of the different structures. MMFF and Density Functional Theory (DFT) with the B3LYP/6-31G basis set were the optimization methods used (Li et al., 2004; Wang et al., 2020). After that, the structures with the lowest possible energy were stored in PDB file format for molecular docking analysis.

2.3 Molecular Docking Investigation

The RCSB Protein Data Bank provided the crystal structure of the protein target, PdxK from *Leishmania donovani*, PDB ID: 6K91 which was used in this investigation (Are et al., 2020). The resulting protein-ligand assembly was generated by removing co-factors, ligands, and related water molecules using the Molegro Virtual Docker (MVD) v6.0 workspace. Any impacted residue can be rebuilt or repaired thanks to MVD. After investigating the binding cavities of the receptors, the one with the biggest volume (398.336) was kept for the receptor. Figure (2) shows the 3D structure of PdxK with the defined binding site. For use in docking simulation, the prepared receptor was then stored in PDB file format (Abdullahi et al., 2022; Edache et al., 2020; Ibrahim et al., 2021). The PDB file format was also used to store the prepared structures of the different chemicals, including the SD. Next, the Pyrx tool AutoDock vina was used to dock the protein with the ligands.

The compounds that were prepared earlier were introduced along with partial charges of Gasteiger and non-polar hydrogen atoms. The torsion angles had unrestricted rotation. To achieve the best docking outcome, a grid box with the center (X = 29.3648Å Y = 1.3484Å Z = 27.9440Å) and dimensions (X = 50.6424Å Y = 46.7480Å Z = 54.4647Å) adjusted to cover the target molecule. A 100-run docking algorithm adjustment was made. Typically, the empirical free energy function and the Lamarckian Genetic Algorithm (LGA) were utilized as the default parameters. The Biovia Discovery Studio Visualizer was utilized to gather and analyze the best postures, which were determined by comparing the poses with the highest binding scores (Fuhrmann et al., 2010; Ugbe et al., 2022c).

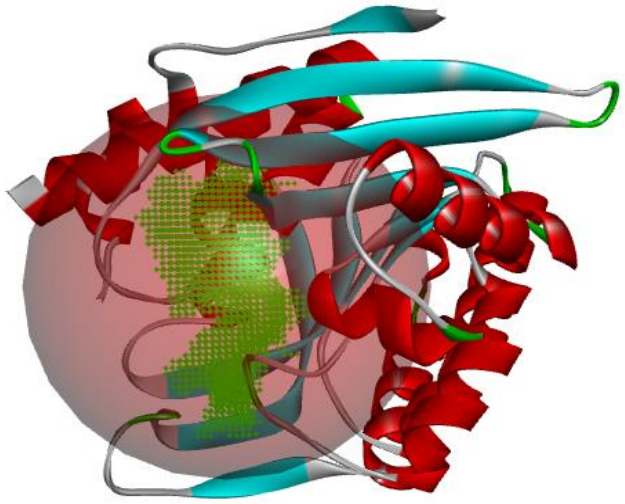

Figure 2: A 3D representation of PdxK showing the defined binding site

2.4 Molecular Dynamics Simulation and MM/GBSA Calculation

The protein-ligand complexes A_6K91, B_6K91, C_6K91, D_6K91, E_6K91, and SD_6K91, which involve lead molecules and SD, were subjected to MD simulation using a combination of the Visual Molecular Dynamics (VMD), Nano-scale Molecular Dynamics (NAMD), and Chemistry at Harvard Macromolecular Mechanics (CHARMM) force field. The input files for the simulation by NAMD were created using the CHARMM-GUI, a well-known web-based tool that makes use of the CHARMM force field (Lee et al., 2016). When solvating the system by fitting it inside a cubic water box, periodic boundary conditions were applied. In an aqueous solution containing potassium chloride salt at a concentration of 0.10M, the proteins were specifically solvated and neutralized (Edache et al., 2022).

Next, in order to stabilize the intricate structures and prevent steric conflicts, energy minimization was carried out. The resultant ion and solvent systems were equilibrated to stabilize the system at 315K and at a constant number of particles, volume, and temperature (NVT ensemble). Additionally, a 1-second time frame was used to stabilize the pressure by maintaining a constant number of particles, pressure, and temperature (NPT ensemble) (Muniba, 2019). The resultant system was then subjected to MD simulation for 100ns (50,000,000 steps), and the data were displayed using VMD and the Biovia Discovery Studio visualizer (Edache et al., 2022; Ugbe et al., 2022d; Ugbe et al., 2024).

Furthermore, using the MD log files produced by NAMD, the MolAICal program was utilized to calculate the ligand-binding affinities via the MM/GBSA technique (Bai et al., 2021). Equations (1) - (3) was used to estimate MM/GBSA (Bai et al., 2021).

$$\Delta G_{bind} = \Delta H - T\Delta S \approx \Delta E_{MM} + \Delta G_{sol} - T\Delta S \quad (1)$$

$$\Delta E_{MM} = \Delta E_{internal} + \Delta E_{ele} + \Delta E_{vdw} \quad (2)$$

$$\Delta G_{sol} = \Delta G_{SA} + \Delta G_{GB} \quad (3)$$

Where the gas phase conformational entropy and MM energy are represented, respectively, by -TΔS and ΔE_{MM}. Electrostatic (E_{ele}), Van der Waal (E_{vdw}), and internal bond, angle, and dihedral energies are all contained in ΔE_{MM}. The solvation-free energy, ΔG_{sol}, is the total of the electrostatic solvation energy, ΔG_{GB}, and the non-electrostatic solvation component, ΔG_{SA}.

2.5 Evaluation of Pharmacokinetic Properties

In the early phases of drug research, pharmacokinetic property prediction is extremely important. This is because pre-clinical research is only accessible to compounds that exhibit strong ADMET and drug-like qualities (Lawal et al., 2021). To assess the drug-likeness and ADMET properties of the various lead compounds and the SD, two free online web servers were used: http://www.swissadme.ch/index.php and http://biosig.unimelb.edu.au/pkcsm, in that order (Pires et al., 2015). The different compounds were supplied in MDL mol file format, which both online servers support. A well-known metric for figuring out a compound's oral bioavailability is Lipinski's Rule of Five (RO5), often known as the Pfizer rule (Lawal et al., 2021; Lipinski et al., 2012).

To determine the studied drugs' oral bioavailability, the RO5 criteria were applied. Molecular Weight (MW), the quantity of Hydrogen Bond Donors (HBD), Hydrogen Bond Acceptors (HBA), lipophilicity indices (MLOGP), the Bioavailability score (BA), and synthetic accessibility were among the physicochemical features of the compounds that were investigated to do this. Equal attention was paid to the distribution and absorption characteristics, such as Central Nervous System (CNS) permeability and Blood-Brain Barrier (BBB) penetration, and Human Intestinal Absorption (HIA). Additionally, studies were conducted on AMES Toxicity, drug total clearance, and excretion features such CYP-3A4 inhibitor/substrate.

3. Results and Discussion

3.1 Molecular Docking Investigation

The strength of each compound's binding to the protein target PdxK was profiled by performing docking research on the five chemicals and the standard drug. Table (1) presents the result of the investigation in terms of binding affinities in kcal/mol. Figure (3) a-f also displays the 2D and 3D representations of their interactions with PdxK. Additionally, Table (2) presents the predicted pharmacological interaction profiles of these compounds with the target protein PdxK.

Table 1: Summary of binding interaction affinities of the lead compounds and Pentamidine with Pyridoxal kinase (PdxK) receptor

S/N	Compound ID	Binding affinity (kcal/mol)
1	A	-7.8
2	B	-10.7
3	C	-10.5
4	D	-9.1
5	E	-8.7
6	SD	-8.1

The effectiveness of the drug's binding to the target macromolecule is determined by the binding affinities of the protein-ligand (drug) interactions. The most energetically stable drug-receptor complex is formed when ligands fit into the target protein pocket well, as shown by the binding energy change (ΔG) being negative (Aniyery et al., 2017). Therefore, the likelihood that a prospective medication candidate will start a protein biochemical activity or reaction increases with the binding energy's negative value (Arun et al., 2016).

Table (2) displays the findings of the docking analysis (binding affinities) between the different compounds and PdxK. It indicates that all compounds, except for compound A, interact more strongly with Pyridoxal kinase than the standard medication (Pentamidine). The binding scores are arranged as follows: B (-10.7) > C (-10.5) > D (-9.1) > E (-8.7) > SD (-8.1) > A (-7.8).

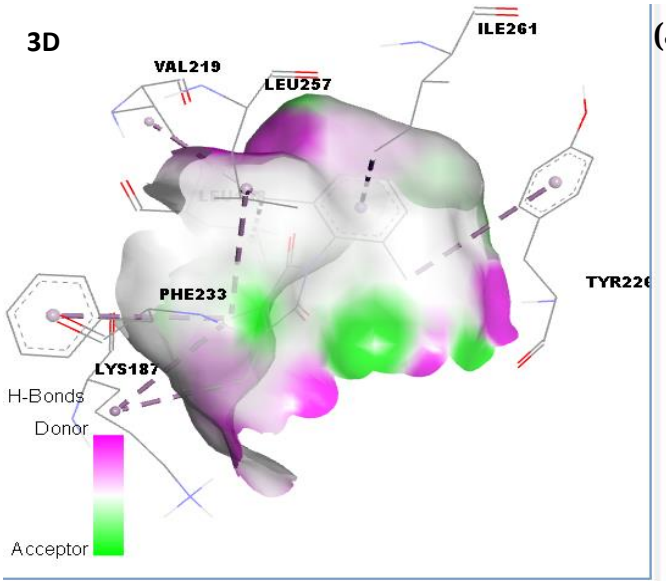

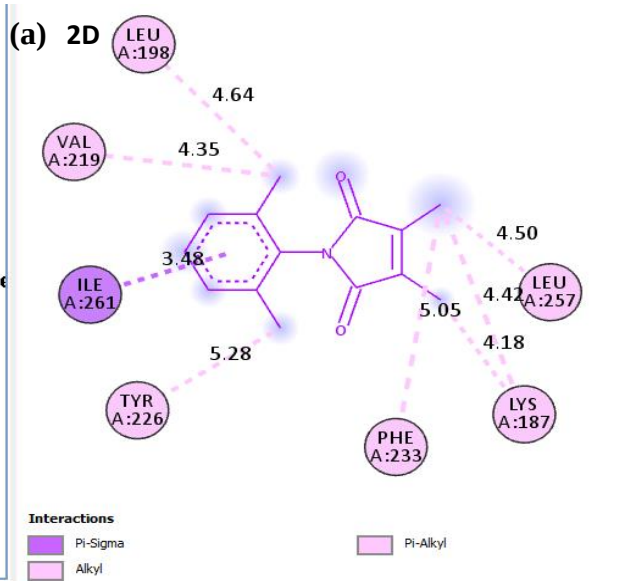

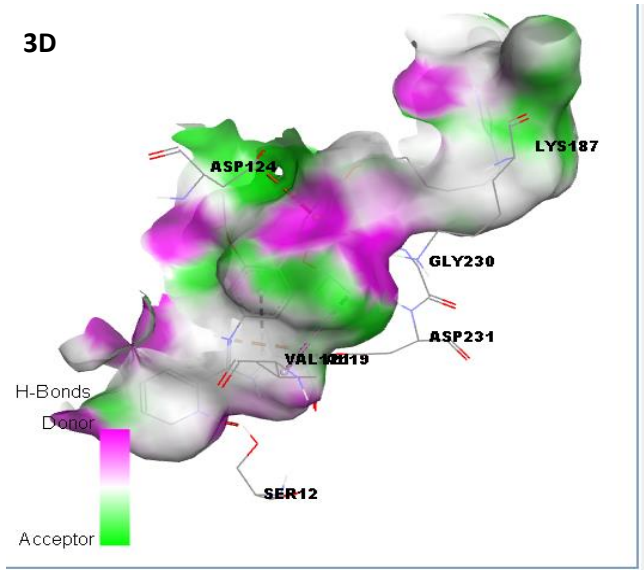

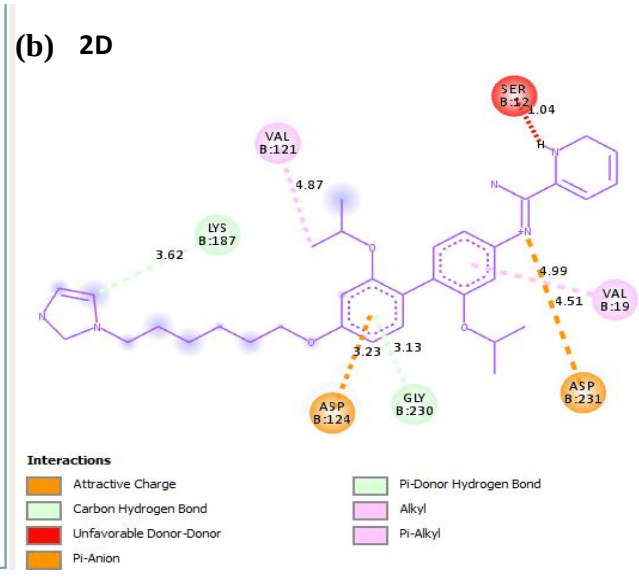

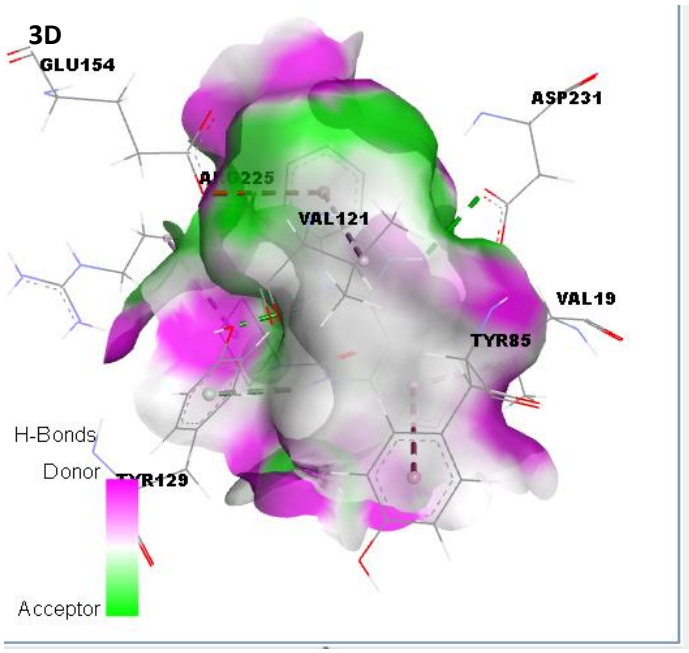
3D
GLU154
ASP231
ARG225
VAL121
VAL19
TYR85
TYR129
H-Bonds
Donor
Acceptor

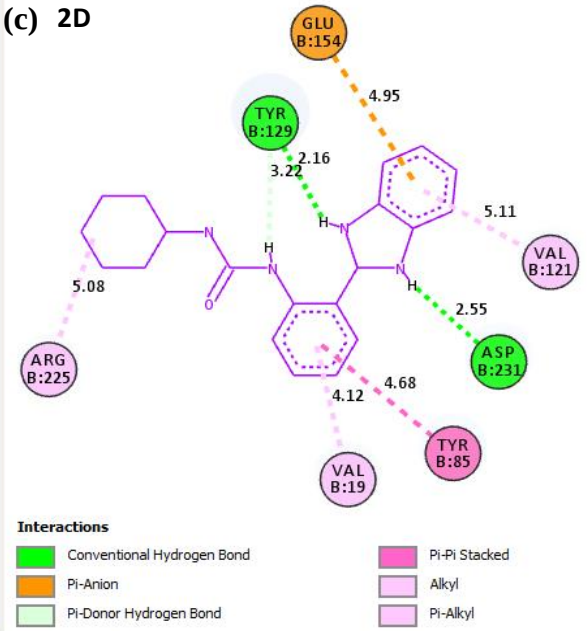
(c) 2D
GLU B:154
TYR B:129
VAL B:121
ASP B:231
ARG B:225
TYR B:85
VAL B:19
4.95
2.16
3.22
5.11
5.08
2.55
4.68
4.12
Interactions
Conventional Hydrogen Bond
Pi-Anion
Pi-Donor Hydrogen Bond
Pi-Pi Stacked
Alkyl
Pi-Alkyl

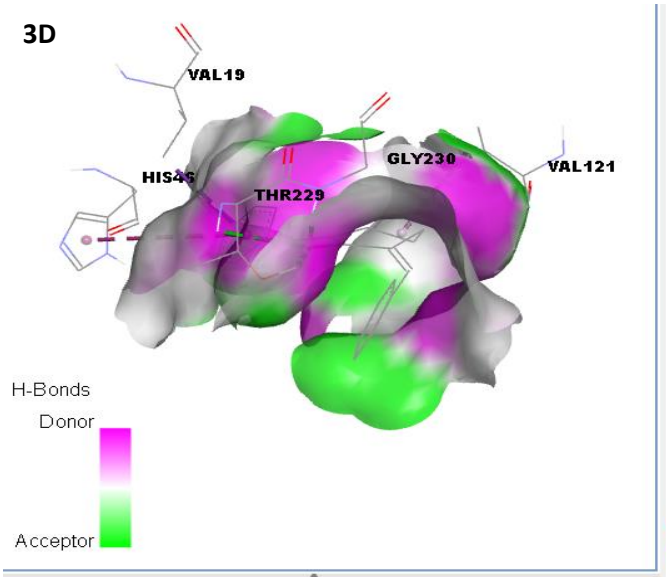
3D
VAL19
HIS46
GLY230
VAL121
THR229
H-Bonds
Donor
Acceptor

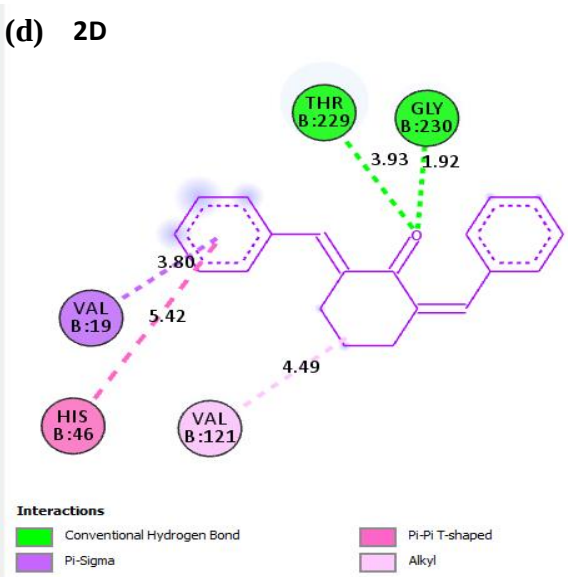
(d) 2D
THR B:229
GLY B:230
VAL B:19
HIS B:46
VAL B:121
3.93
1.92
3.80
5.42
4.49
Interactions
Conventional Hydrogen Bond
Pi-Sigma
Pi-Pi T-shaped
Alkyl

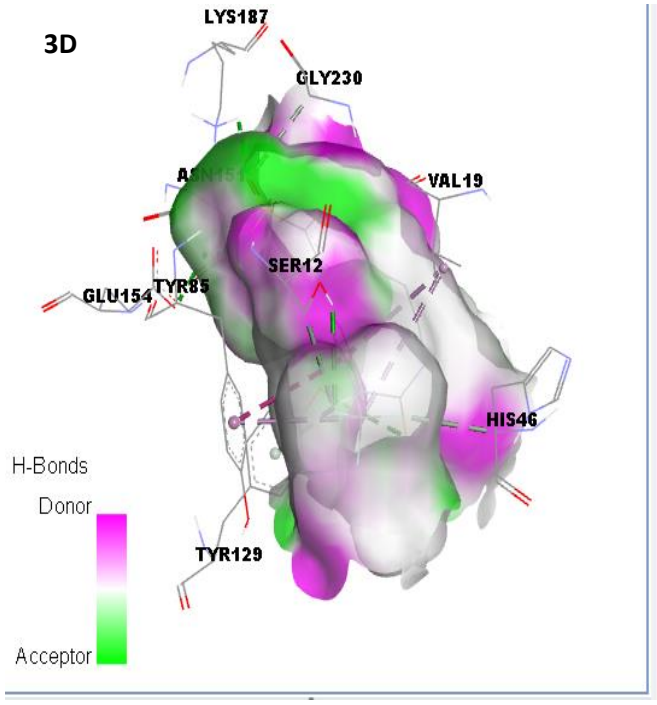
3D
LYS187
GLY230
VAL19
SER12
GLU154
TYR85
HIS46
TYR129
H-Bonds
Donor
Acceptor

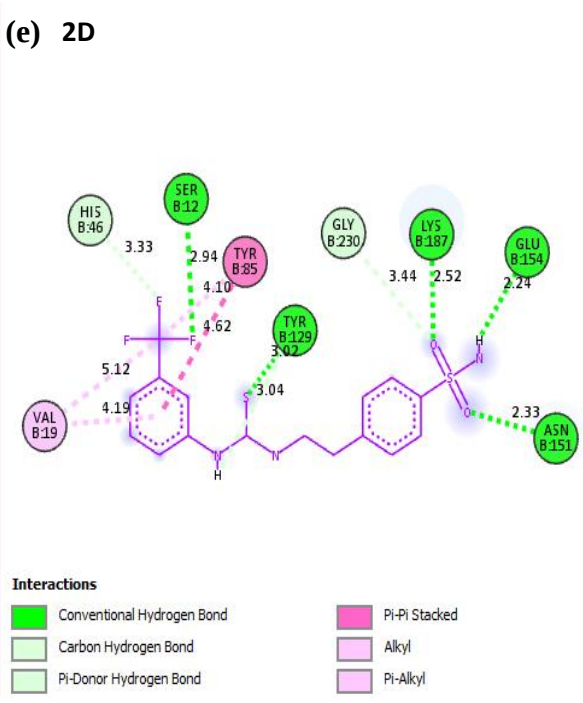
(e) 2D
HIS B:46
SER B:12
GLY B:230
LYS B:187
GLU B:154
TYR B:85
TYR B:129
VAL B:19
ASN B:151
3.33
2.94
4.10
4.62
3.44
2.52
2.24
5.12
4.19
3.04
2.33
Interactions
Conventional Hydrogen Bond
Carbon Hydrogen Bond
Pi-Donor Hydrogen Bond
Pi-Pi Stacked
Alkyl
Pi-Alkyl

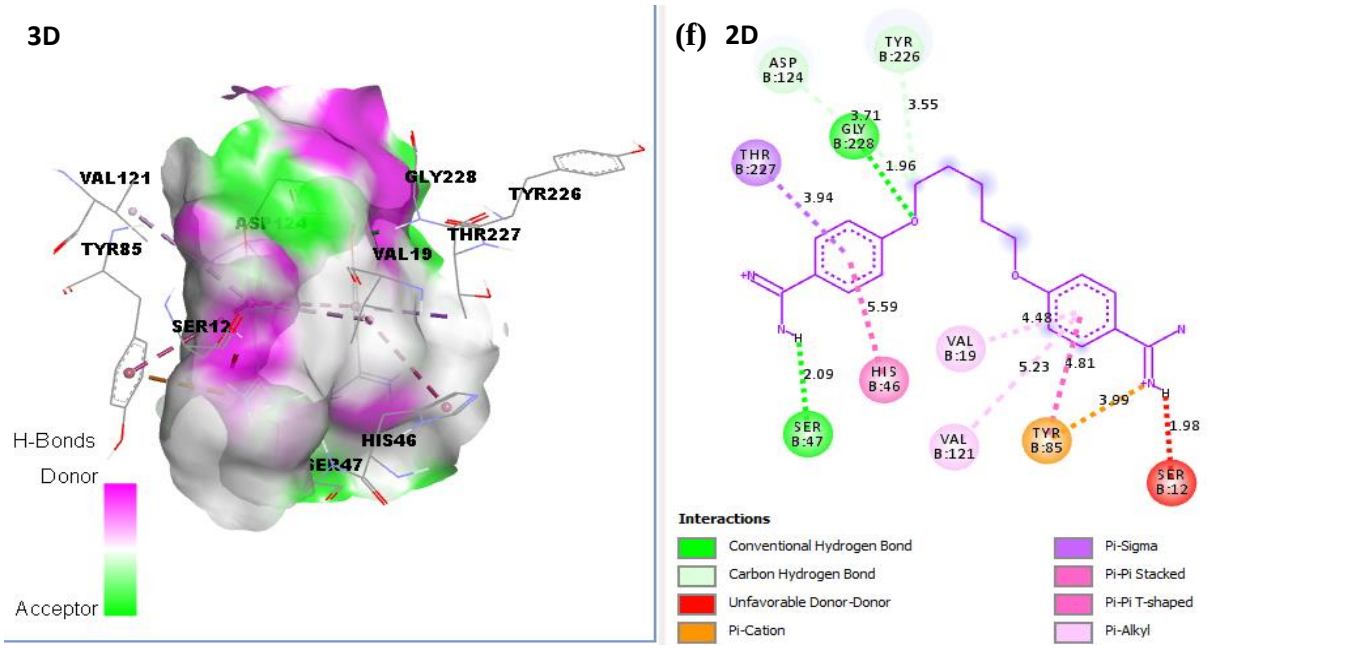

Figure 3: 3D and 2D view of the interactions between PdxK and the various anti-leishmanial compounds (a) A_6K91 (b) B_6K91 (c) C_6K91 (d) D_6K91 (e) E_6K91 (f) SD_6K91

The interactions between the lead molecules, SD, and the receptor are visualized in 2D and 3D forms as displayed in Figure (3) a-f. Some important interactions in drug and receptor binding were visible including hydrophobic, electrostatic, and hydrogen bonding interactions. To make drug-receptor binding reversible, these interactions are necessary. To aid the stabilization of docked complexes and improve ligand binding affinity at the ligand-receptor interface, H-bonds and hydrophobic interactions are essential (Nipun et al., 2021). Furthermore, H-bond is a key factor in regulating how selective ligand binding is (Imberty et al., 1991).

Table 2: Predicted pharmacological interaction profiles of the lead compounds and standard drug pentamidine with PdxK

Comp. ID	Hydrogen bond Interactions			Electrostatic/Hydrophobic/Van der Waal interactions/Others
	Amino acid	Type	Distance (Å)	
A	-	-	-	VAL-219 (alkyl), LEU-198 (alkyl), ILE-261 (π-alkyl), TYR-226 (alkyl), PHE-233 (alkyl), LYS-187 (alkyl), LEU-257 (alkyl)
B	THR-229	Conventional	1.95	ASP-124 (π-anion), TYR-85 (π- π stacked), VAL-121 (alkyl), π-alkyl (LEU-43, VAL-41, VAL-19, MET-254, LEU-257) and unfavourable donor-donor clash with SER-47
	GLN-258	Conventional	2.78	
	SER-47	Conventional	2.42	
	HIS-46	C – H	2.95	
	ASP-124	C – H	2.69	
	GLY-230	π-donor	3.18	
C	TYR-129	Conventional	2.16	GLU-154 (π-anion), TYR-85 (π- π stacked), ARG-225 (alkyl), π-alkyl (VAL-121, VAL-19), VAL-121 (π-sigma)
	ASP-231	Conventional	2.55	
	TYR-129	π –donor	3.22	
D	THR-229	Conventional	2.52, 2.56	π-π T shaped (HIS-46), π-sigma (VAL-19), alkyl (VAL-121)
	GLY-230	Conventional	1.93	
E	ASN-151	Conventional	2.33	TYR-85 (pi-pi stacked), VAL-19 (Alkyl), VAL-19 (pi-alkyl), HIS-46 (Flourine)
	GLU-154	Conventional	2.24	
	LYS-187	Conventional	2.52	
	SER-12	Conventional	2.94	
	TYR-129	Conventional	3.02	
	GLY-230	C-H	3.44	
	SER-12	C-H	3.33	
	TYR-129	π-donor	3.04	
SD	SER-47	Conventional	2.52	VAL-19 (π-alkyl) and unfavorable donor-donor clash with SER-12.
	THR-229	Conventional	2.53	
	TYR-129	C-H	2.36	
	GLY-228	π-donor	2.39	

It is evident from the binding interaction profile of A with PdxK (Figure (3a)) that hydrogen bond interactions were absent from the binding interactions, which were solely defined by electrostatic and hydrophobic interactions. This could be explained by the steric hindrances caused by the chloro groups on the pyrrole ring and the side chain methyl groups on the phenyl ring, which prevent the carbonyl groups from forming

hydrogen bonds with amino acid residues. Except for ILE-261, which binds electrostatically to the π electron system of compound 24's benzene ring via its alkyl group, the majority of the observed contacts were hydrophobic (alkyl type).

Several interactions were visible from the binding profile of B with PdxK (Figure (3b)). Three (3) conventional H-bonds were formed involving GLN-258 (interaction distance of 2.78 Å), THR-229 (1.95 Å), and SER-47 (2.42 Å), Two (2) carbon-hydrogen (C-H) bonds were visible with HIS-46 and ASP-124, a π-donor hydrogen bond with GLY-230, π-anion electrostatic interaction with ASP-124, and several hydrophobic interactions. Compound C was said to interact very adequately with the target receptor (PdxK) as shown by the presence of H-bonding, hydrophobic interactions, and electrostatic interactions (Figure (3c)). Some of the observed interactions include Two (2) conventional H-bonds with TYR-129 and ASP-231 at 2.16 Å and 2.55 Å respectively, and π-donor H-bond with TYR-129 at 3.22 Å. GLU-154 was involved in π-anion electrostatic interaction with the compound, while the remaining interactions were hydrophobic including TYR-85 (π-π stacked), ARG-225 (alkyl), π-alkyl (VAL-121 and VAL-19), and π-sigma (VAL-121).

The binding profile of D with PdxK (Figure 2d) involved a total of Three (3) conventional H-bonds and up to Three (3) hydrophobic interactions. The carbonyl group (C=O) oxygen of the cyclohexanone ring played a significant role in the formation of 3 conventional H-bonds with THR-229 at interaction distances of 2.52Å and 2.56Å, and GLY-230 at 1.93Å. The hydrophobic interactions include π-π T-shaped and π-sigma with HIS-46 and VAL-19 respectively via one of the phenyl π-electron systems, and alkyl interaction with VAL-121 via C-4 carbon of the cyclohexanone ring system.

For compound E, the binding interaction profile was characterized by H-bonding and hydrophobic interactions, with H-bonding being dominant (Figure (3e)). Five (5) conventional H-bonds were visible with ASN-151, GLU-154, LYS-187, SER-12, and TYR-129 at interaction distances of 2.33 Å, 2.24 Å, 2.52 Å, 2.94 Å, and 3.02 Å respectively. Also observed were C-H bonds with GLY-230 and SER-12 at 3.44 Å and 3.33 Å respectively, and π-donor H-bond with TYR-129 (3.04 Å). Other interactions include Fluorine (HIS-46), and hydrophobic interactions; π-π stacked (TYR-85), Alkyl (VAL-19), and π-alkyl (VAL-19).

Although the interaction profile of the standard drug (Figure (3f)) was equally characterized by important interactions in drug-receptor binding, an unfavorable acceptor-acceptor clash was conspicuous with SER-47. Based on the pharmacological interaction study, it was obvious that the lead compounds demonstrated strong binding interactions with the target protein.

3.2 Molecular Dynamics Simulation and MM/GBSA Calculation

The MD simulation was performed on the lead molecules and the standard drug pentamidine in a complex with the target protein (6K91) to study their interaction kinetics. Figure (4 a-c) showed the results of the simulations as plots of Root-Mean-Square Deviation (RMSD), Root-Mean-Square Fluctuation (RMSF), and Radius of gyration (Rg) versus the time in nanoseconds (ns) respectively. The 2D representations of the binding interactions after the simulation are displayed in Figure (5 a-f) for the lead molecules and the standard drug respectively. Furthermore, the binding free energies of interactions (MM/GBSA) were calculated for the various complexes and presented in Table (3).

The stability of protein-ligand complexes can be qualitatively indicated by two most important indicators; the root mean square deviation (RMSD) and the root mean square fluctuation (RMSF) (Eltayb et al., 2023). RMSD values will indicate how structures and parts of structures change over time as compared to the starting point. A large RMSD value shows a great deviation in structural changes compared to the structure at the starting point and thus indicates less stability of the complex. RMSD is typically plotted vs. time (Abdalla et al., 2022). RMSF on the other hand is a calculation of individual residue flexibility, or how much a particular residue moves (fluctuates) during a simulation.

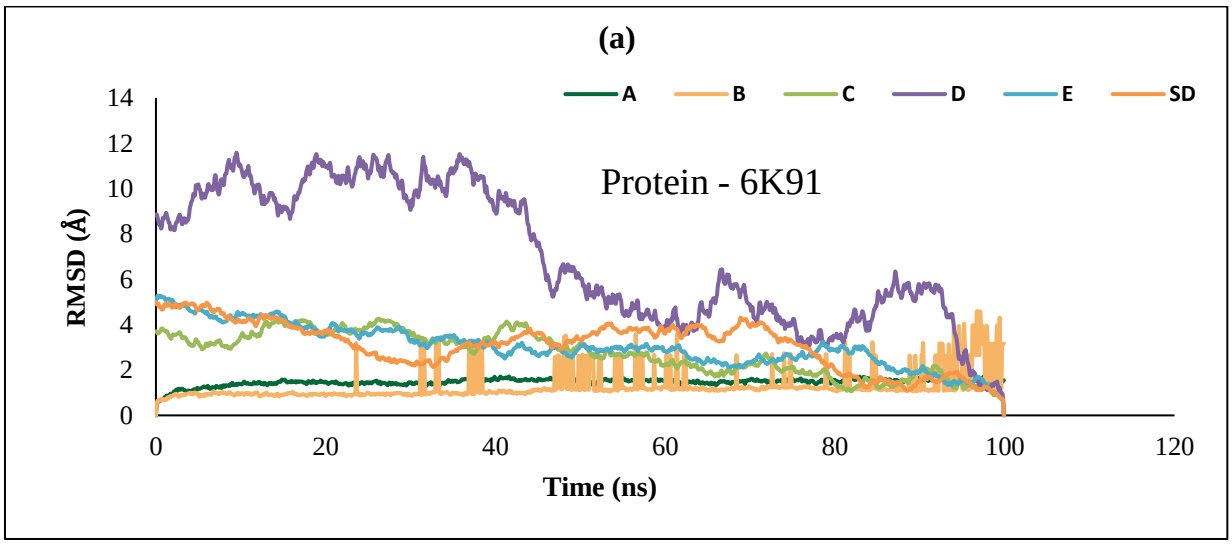

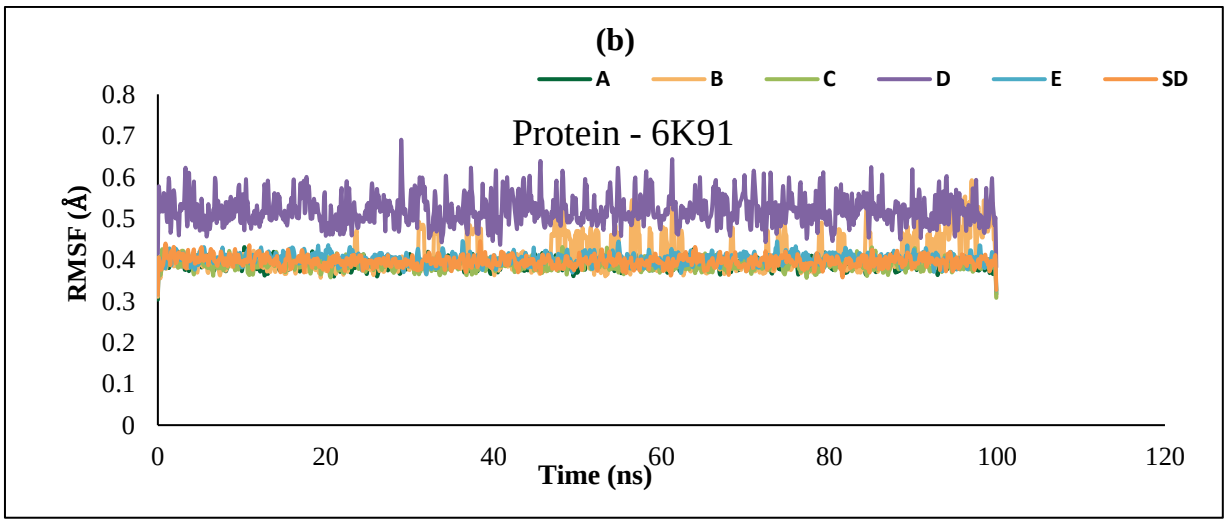

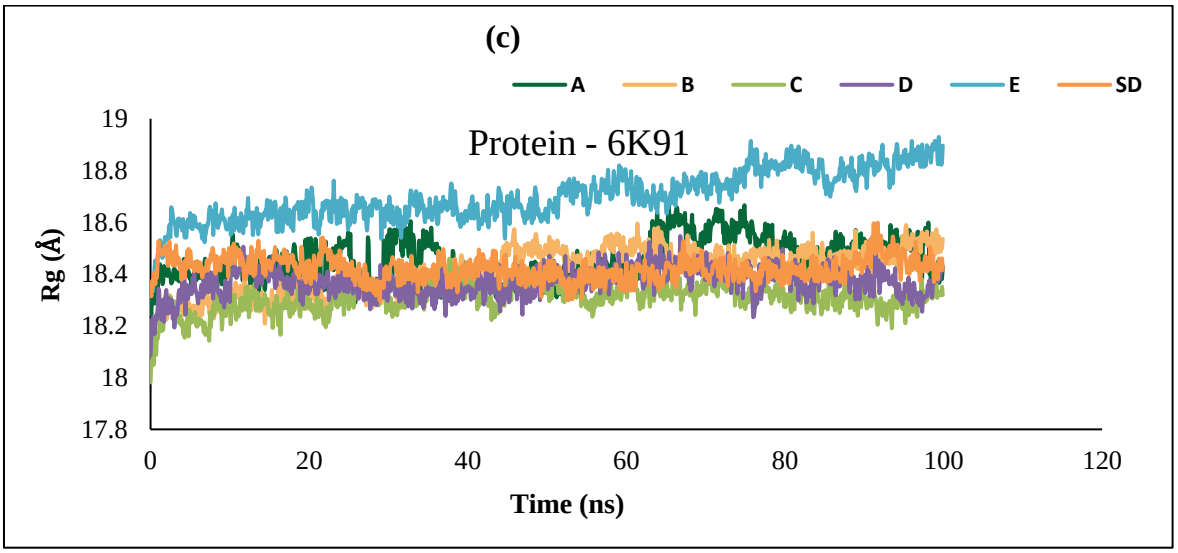

Figure 4: MD simulation study of the various compounds with PdxK (a) Plot of RMSD versus time (ns) (b) Plot of RMSF versus time (ns) (c) plot of Rg versus time (ns)

The average RMSD values for the complexes (Figure (4a)); A_6K91, B_6K91, C_6K91, D_6K91, E_6K91, and SD_6K91 were estimated at 1.4724 Å, 1.2990 Å, 2.74078Å, 6.9874Å, 3.0552 Å, and 3.1194 Å respectively, which showed that B and D had the least and greatest deviation from the original conformation respectively during the trajectory. The RMSF plot in Figure 3b showed that the flexibilities of the protein residues were almost constant during the trajectory, an indication of the stability of the interactions during the simulation, with D_6K91 showing a relatively higher fluctuation.

The Rg is a measure of the degree of protein's compactness during the trajectory. Decreasing Rg indicates reducing residues' flexibilities and more stability for the protein. Throughout the trajectory, the Rg varies between 18.244 Å and 18.667 Å for 2A_6K91, 18.089 Å and 18.595 Å for B_6K91, 18.05 Å and 18.50 Å for C_6K91, 18.10 Å and 18.80 Å for D_6K91, 18.30 Å and 18.90 Å for E_6K91, and between 18.2967 Å and 18.5987 Å for SD_6K91, all of which were not more than a difference of 0.70 Å, connoting slight changes in the protein compactness as the simulation progresses, and which means the stability of the complexes (Figure (4c)). Based on the Rg values, the stability of the complexes follows the order; SD > A > C > B > E > D, with D showing the least stability.

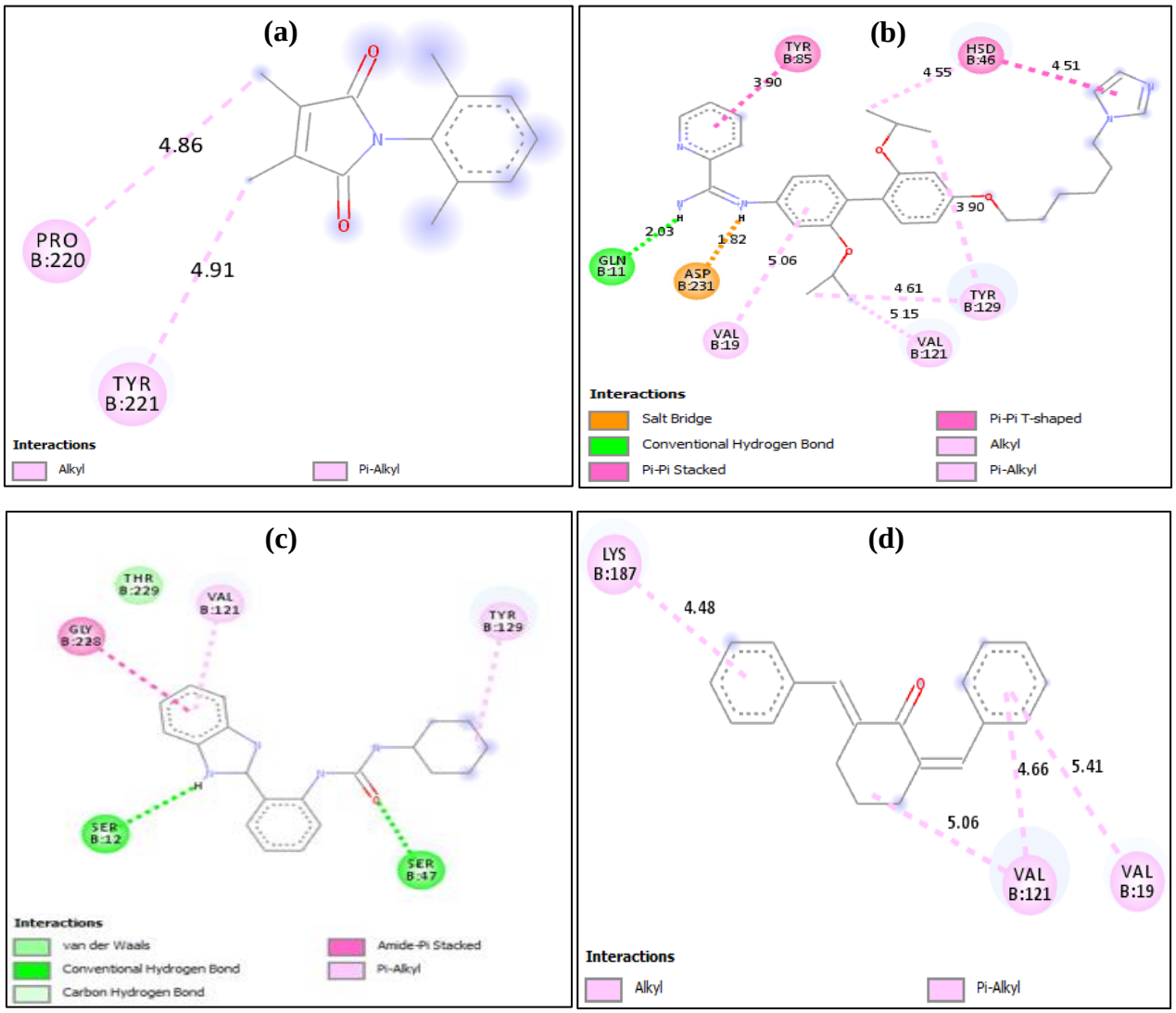

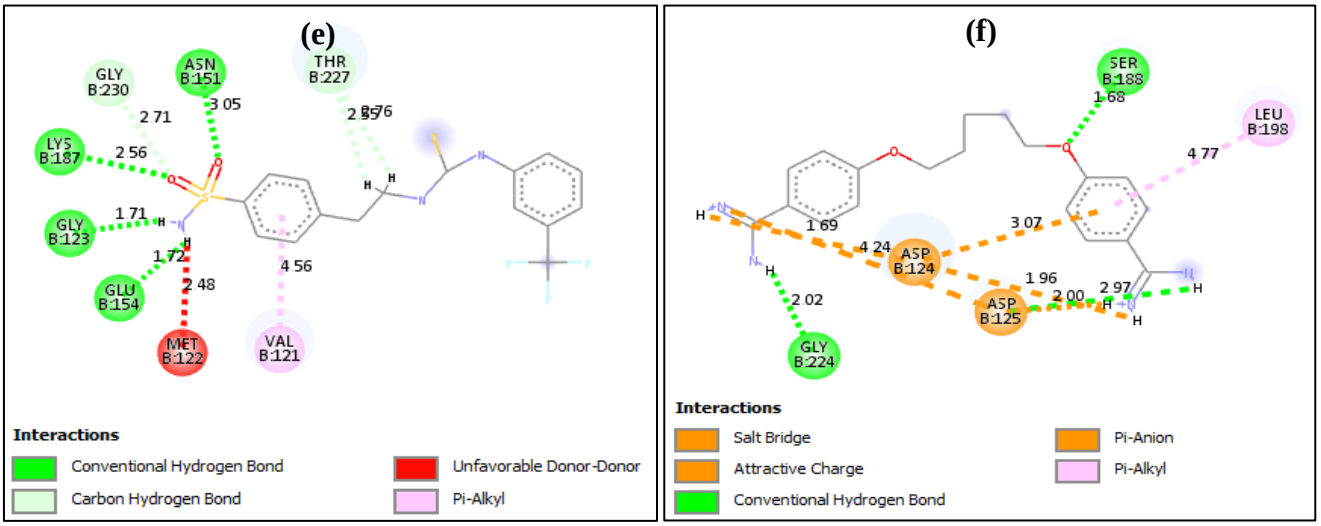

Figure 5: 2D view of the binding interactions between Pyridoxal kinase and the anti-leishmanial compounds after MD simulation; (a) A (b) B (c) C (d) D (e) E (f) SD

It is important to note that when drugs and receptors interact, they do so in a real dynamic system. Hence, it became necessary to examine how the various complexes behave in a dynamically simulated system, which can be likened to the real dynamic system. To further ascertain the stability of the protein-ligand interactions after the MD simulation, the binding interactions were visualized on Biovia Discovery Studio and reported in Figure (5 a-f). The binding interaction patterns of the non-simulated A_6K91 (Figure (3a)) and simulated A_6K91 (Figure (5a)) were majorly characterized by hydrophobic interactions, with several interactions being lost in the simulated complex. Although characterized by loss of interactions, the observed hydrophobic interactions are equally important in drug-receptor binding.

The interaction profiles of the simulated complex B_6K91 (Figure (5b)) were characterized by several interactions including H-bonding, electrostatic, and hydrophobic interactions, all important in drug-receptor binding. This confirmed the stability of the complex during the trajectory. Interestingly too, no unfavorable steric bumps or clashes were visible in the B_6K91 interaction profile. Also, the binding interaction profile of the simulated complex C_6K91 (Figure (5c)) deviated only slightly from that of the non-simulated complex (Figure (3c)) regarding the number of interactions formed. It also became obvious that the conventional H-bond interactions were lost following the dynamic simulation of the complex D_6K91. Only hydrophobic interactions (VAL-19, VAL-121, and LYS-187) were visible.

The binding interaction profiles of the simulated complex E_6K91 (Figure (5e)) showed very similar interactions with those of the non-simulated complex (Figure (3e)), especially regarding the conventional H-bonding interactions. For SD_6K91 (Figure (5f)), conventional hydrogen bonding, hydrophobic, and electrostatic interactions were conspicuous. Moreover, no unfavorable steric bumps or clashes were visible. On the whole, the binding profiles of the various complexes after MD simulation suggest the great stability they exhibited in the order; B > SD > C > E > D > A.

Table 3: Binding free energy parameters of the various protein-ligand complexes

Simulated complex	Energy Parameters (kcal/mol)			
	ΔE(internal)	ΔE(electrostatic) + ΔG(solvation)	ΔE (Van der Waal)	ΔG binding (MM/GBSA)
A_6K91	-2.9377	6.2853	0.5251	3.8727 ± 0.4485
B_6K91	40.7588	-109.3867	-19.5936	-88.2216 ± 0.6948
C_6K91	-3.7128	18.0197	-40.2733	-25.9665 ± 0.5391
D_6K91	12.0423	-28.549	-40.9152	-57.4219 ± 0.3845
E_6K91	8.9800	-15.5191	-44.7127	-51.2518 ± 0.4857
SD_6K91	-34.5718	-1.5058	-20.7063	-56.7839 ± 0.2691

The results of binding free energies (MM/GBSA) estimated for the various complexes studied were earlier reported in Table (3). The negative values of the estimated binding free energies of these complexes except A_6K91 (3.8727 ± 0.4485 kcal/mol) indicate the favorability of the ligand-protein binding. Also, the magnitudes of MM/GBSA in kcal/mol for the various anti-leishmanial compounds are in the order; B_6K91 (-88.2216) > D_6K91 (-57.4219) > SD_6K91 (-56.7839) > E_6K91 (-51.2518) > C_6K91 (-25.9665) > A_6K91 (unfavorable).

Furthermore, the estimated MM/GBSA for the studied complexes compared favorably well with those of other protein-ligand complexes reported elsewhere (Table (4)). Therefore, the various compounds except A have demonstrated the potential to arrest the target enzyme examined (6K91).

Table 4: Comparative study of binding free energy (MM/GBSA) values of different ligand-protein complexes

Inhibitor	Receptor	MMGBSA (kcal/mol)	Author (s)
B	Pyridoxal kinase	-88.2216 ± 0.6948	This study
D	Pyridoxal kinase	-57.4219 ± 0.3845	This study
E	Pyridoxal kinase	-51.2518 ± 0.4857	This study
30	Chlamydia trachomatis protein	-40.2363 ± 0.3449	Edache et al., 2023a
36	SARS-CoV-2 protein	-40.8176 ± 0.5498	Edache et al., 2023b
178	ALK tyrosine kinase	-52.5000 ± 3.0000	Jawarkar et al., 2022
172	ALK tyrosine kinase	−49.4000 ± 4.20000	Jawarkar et al., 2022
Glycyrrhizin	SARS-CoV-2 protein	−57.0000 ± 8.0000	Zamzami, 2023
C-14	SARS-CoV-2 RdRp	−46.9500 ± 6.3000	Elfiky et al., 2022

3.3 Evaluation of Pharmacokinetic Properties

The results of the drug-likeness analysis conducted on the various compounds were presented in Table (5), while Table (6) showed their predicted ADMET properties.

Table 5: Predicted drug-likeness properties of the various compounds

Comp. ID	Binding affinity	MW (g/mol)	MLOGP	HBD	HBA	RO5 Violation	BA	Drug-likeness
A	-7.8	270.11	2.22	0	2	0	0.55	YES
B	-8.3	555.71	3.21	2	6	1	0.55	YES
C	-10.5	334.41	3.37	3	2	0	0.55	YES
D	-9.1	274.36	4.16	0	1	1	0.55	YES
E	-8.9	450.34	2.51	3	6	0	0.55	YES
SD	-8.1	340.42	2.80	4	4	0	0.55	YES

The drug-likeness properties of the compounds were predicted based on the provisions of Lipinski's 'rule of 5', which states that poor drug absorption or permeation is more likely associated with Hydrogen Bond Donors (HBD) > 5, Hydrogen Bond Acceptors (HBA) > 10, Molecular Weight (MW) > 500, and lipophilicity (MLOGP > 4.15) (Lipinski et al., 2012). Molecules satisfying at least three of the four requirements are said to obey Lipinski's rule for oral bioavailability (Ibrahim et al., 2021; Lawal et al., 2021). In the present study, all the compounds (Table (5)) perfectly obeyed Lipinski's rule less B with one violation (MW > 500) and D (MLOGP > 4.15). Based on the predicted drug-likeness parameters, all the tested compounds were said to be orally bioavailable and compared well with the tested standard drug.

Table 6: Predicted ADMET properties of the various compounds

Comp ID	Absorption	Distribution		Metabolism		Excretion	Toxicity
	HIA (%)	BBB	CNS	CYP-34A		Total clearance	AMES
		Log BB	Log PS	Substrate	Inhibitor		
A	95.75	0.329	-2.136	NO	NO	-0.029	NO
B	100.0	-0.70	-2.29	YES	YES	0.848	NO
C	78.07	-0.70	-1.81	NO	NO	0.893	NO
D	94.61	0.54	-1.15	YES	NO	0.163	NO
E	88.55	-0.997	-2.779	YES	NO	2.072	NO
SD	77.04	-0.905	-2.941	NO	NO	0.85	NO

Table (6) showed a very high Human Intestinal Absorption (HIA) of greater than 75 % for all the compounds examined, which is well above the 30% HIA threshold mark. The Blood-Brain Barrier (BBB) and Central Nervous System (CNS) penetration is possible if the logarithmic ratio of brain to plasma drug concentration (logBB) is greater than 0.3 and the blood-brain permeability-surface area product (logPS) is greater than -2 respectively (Umar et al., 2023). A logBB of less than 0.3 is poorly distributed to the brain, whereas those with logPS of less than -2 are not able to penetrate the CNS (Pires et al., 2015). Consequently, logBB for all tested molecules is less than 0.3, meaning they do not readily permeate the BBB except A and D with logBB above 0.3. Additionally, only C and D were predicted to permeate the CNS since they showed log PS > -2.

Furthermore, B alone is both a substrate and an inhibitor of Cytochrome P450 (CYP-3A4), an enzyme essential for drug metabolism in the body (Umar et al., 2023). Also, only A, C, and SD are neither substrates nor inhibitors of CYP-3A4, while D and E are substrates of the enzyme only. The total clearance for a drug molecule in the body for the tested molecules falls within the acceptable range. The AMES toxicity test was conducted for all the selected compounds, all of which showed a negative AMES toxicity, indicating that the compounds are non-mutagenic and cannot act as carcinogens (Abdullahi et al., 2023). Considering the predicted ADMET parameters, the various compounds were said to possess good ADMET properties, while also comparing favorably well with the standard drug.

4. Conclusion

This comparative study evaluated the anti-leishmanial potential of some selected lead compounds by employing the *in-silico* approach of molecular docking, MD simulation, and pharmacokinetic profiling. This reduces the time and huge cost associated with the drug discovery process. The molecular docking investigation conducted between the lead compounds and the target receptor, Pyridoxal Kinase (PdxK) showed that the various compounds bind well into PdxK's cavities with binding affinities in the order; B (-10.7 kcal/mol) > C (-10.5) > D (-9.1) > E (-8.7) > SD (-8.1) > A (-7.8 kcal/mol), which identified B as the most active molecule forming the more energetically stable complex (B_6K91). The MD simulation revealed B_6K91 as having the most stable interactions with an MM/GBSA value of -88.2216 ± 0.6948 kcal/mol, while A_6K91 showed unstable interactions with an unfavorable MM/GBSA value of 3.8727 ± 0.4485. In addition, the various molecules were said to be orally bioavailable and showed good pharmacokinetic properties, comparing favorably well with the standard drug (Pentamidine). Based on the five classes of anti-leishmanial compounds evaluated, the arylimidamide-Azole hybrid (compound B) showed the best drug attributes and is therefore suggested for development and further evaluation as a potential drug candidate for the treatment of leishmaniasis.

Acknowledgments

The authors sincerely acknowledge G.F.S. Harrison Quantum Chemistry Research Group, Ahmadu Bello University Zaria's support and mentorship.

Author's Contributions

FA Ugbe and EI Edache conceived and designed the study. FA Ugbe, AM Ayuba, and EI Edache conducted the study. FA Ugbe, A Jibrin, and OT Amusan drafted the manuscript. AM Ayuba and A Jibrin conducted the technical editing. All authors read and approved the final manuscript.

Funding

This research did not receive any specific grant from funding agencies in the public, commercial, or not-for-profit sectors.

Competing Interests

The authors declare that they have no competing interests.

References

Abdalla, M., Eltayb, W.A., El-Arabey, A.A., Singh, K. and Jiang, X., 2022. Molecular dynamic study of SARS-CoV-2 with various S protein mutations and their effect on thermodynamic properties. Computers in Biology and Medicine, 141, Pp. 105025.

Abdelhameed, A., Feng, M., Joice, A.C., Zywot, E.M., Jin, Y., La Rosa, C., Liao, X., Meeds, H.L., Kim, Y., Li, J. and McElroy, C.A., 2021. Synthesis and

Antileishmanial Evaluation of Arylimidamide–Azole Hybrids Containing a Phenoxyalkyl Linker. ACS infectious diseases, 7 (7), Pp. 1901-1922.

Abdullahi, S.H., Uzairu, A., Shallangwa, G.A., Uba, S. and Umar, A.B., 2022. In-silico activity prediction, structure-based drug design, molecular docking and pharmacokinetic studies of selected quinazoline derivatives for their antiproliferative activity against triple negative breast cancer (MDA-MB231) cell line. Bulletin of the National Research Centre, 46 (1), Pp. 2. https://doi.org/10.1186/s42269-021-00690-z

Abdullahi, S.H., Uzairu, A., Shallangwa, G.A., Uba, S., and Umar, A.B., 2023. Pharmacokinetic profiling of quinazoline-4 (3H)-one analogs as EGFR inhibitors: 3D-QSAR modeling, molecular docking studies and the design of therapeutic agents. Journal of Taibah University Medical Sciences, 18 (5), Pp. 1018-1029.

Adeniji, S.E., Arthur, D.E., Abdullahi, M., Abdullahi, A., and Ugbe, F.A., 2020. Computer-aided modeling of triazole analogues, docking studies of the compounds on DNA gyrase enzyme and design of new hypothetical compounds with efficient activities. Journal of Biomolecular Structure and Dynamics, 40 (9), Pp. 4004-4020.https://doi.org/10.1080/07391102.2020.1852963

Akhoon, S.A., Naqvi, T., Nisar, S., and Rizvi, M.A., 2015. Synthetic organo-selenium compounds in medicinal domain. Asian Journal of Chemistry, 27 (8), Pp. 2745.

Al-Tamimi, A.M.S., Etxebeste-Mitxeltorena, M., Sanmartin, C., Jimenez-Ruiz, A., Syrjänen, L., Parkkila, S., Selleri, S., Carta, F., Angeli, A., and Supuran, C.T., 2019. Discovery of new organoselenium compounds as antileishmanial agents. Bioorganic Chemistry, 86, Pp. 339-345. https://doi.org/10.1016/j.bioorg.2019.01.069

Aniyery, R.B., Gupta, A., and Singh, P., 2017. In-vitro and in silico antimicrobial study of stannane of pyridoxal 5-phosphate. Int J Pharm Pharm Sci., 9 (2), Pp. 145-53.

Are, S., Gatreddi, S., Jakkula, P., and Qureshi, I.A., 2020. Structural attributes and substrate specificity of pyridoxal kinase from Leishmania donovani. International journal of biological macromolecules, 152, Pp. 812-827.https://doi.org/10.1016/j.ijbiomac.2020.02.257

Arun Kumar, A.K., Sharmila, R., Akila, K., and Jaikumar, B., 2016. In-silico approach for the assessment of oral cancer property on Limonia acidissima.

Ashok, P., Chander, S., Smith, T.K. and Sankaranarayanan, M., 2018. Design, synthesis and biological evaluation of piperazinyl-β-carbolinederivatives as anti-leishmanial agents. European Journal of medicinal chemistry, 150, Pp. 559-566. https://doi.org/10.1016/j.ejmech.2018.03.022

Bai, Q., Tan, S., Xu, T., Liu, H., Huang, J. and Yao, X., 2021. MolAICal: a soft tool for 3D drug design of protein targets by artificial intelligence and classical algorithm. Briefings in bioinformatics, 22 (3), Pp. 161.

Bekhit, A.A., Lodebo, E.T., Hymete, A., Ragab, H.M., Bekhit, S.A., Amagase, K., Batubara, A., Abourehab, M.A., Bekhit, A.E.D.A. and Ibrahim, T.M., 2022. New pyrazolylpyrazoline derivatives as dual acting antimalarial-antileishamanial agents: synthesis, biological evaluation and molecular modelling simulations. Journal of enzyme inhibition and medicinal chemistry, 37 (1), Pp. 2320-2333. https://doi.org/10.1080/14756366.2022.2117316

Bjørklund, G., Shanaida, M., Lysiuk, R., Antonyak, H., Klishch, I., Shanaida, V., and Peana, M., 2022. Selenium: an antioxidant with a critical role in anti-aging. Molecules, 27 (19), Pp. 6613. https://doi.org/10.3390/molecules27196613

Chandru, H., Sharada, A.C., Bettadaiah, B.K., Kumar, C.A., Rangappa, K.S., and Jayashree, K., 2007. In vivo growth inhibitory and anti-angiogenic effects of synthetic novel dienone cyclopropoxy curcumin analogs on mouse Ehrlich ascites tumor. Bioorganic and medicinal chemistry, 15 (24), Pp. 7696-7703.

Chen, X.L., Zhang, L.J., Li, F.G., Fan, Y.X., Wang, W.P., Li, B.J. and Shen, Y.C., 2015. Synthesis and antifungal evaluation of a series of maleimides. Pest management science, 71 (3), Pp. 433-440.

Din, Z.U., Trapp, M.A., de Medeiros, L.S., Lazarin-Bidoia, D., Garcia, F.P., Peron, F., Nakamura, C.V., Rodriguez, I.C., Wadood, A., and Rodrigues-Filho, E., 2018. Symmetrical and unsymmetrical substituted 2, 5-diarylidene cyclohexanones as anti-parasitic compounds. European Journal of Medicinal Chemistry, 155, Pp. 596-608.

Dominiak, A., Wilkaniec, A., and Adamczyk, A., 2016. Selenium in the therapy of neurological diseases. Where is it going?. Current neuropharmacology, 14 (3), Pp. 282-299. https://doi.org/10.2174/1570159x14666151223100011

Edache, E.I., Dawi, H.A., and Ugbe, F.A., 2023b. 3D-QSAR, molecular docking, molecular dynamics simulations and structural studies of some selected inhibitors of the glycoprotein (GPC) of Lassa virus. J Appl Organomet Chem, 3 (3), Pp. 224-244.

Edache, E.I., Uzairu, A., Mamza, P.A., and Shallangwa, G.A., 2022. Theoretical investigation of the cooperation of iminoguanidine with the enzymes-binding domain of covid-19 and bacterial lysozyme inhibitors and their pharmacokinetic properties. Journal of the Mexican Chemical Society, 66 (4), Pp. 513-542. https://doi.org/10.29356/jmcs.v66i4.1726

Edache, E.I., Uzairu, A., Mamza, P.A., Shallangwa, G.A., Azam, M. and Min, K., 2023a. Methimazole and propylthiouracil design as a drug for anti-graves' disease: Structural studies, Hirshfeld surface analysis, DFT calculations, molecular docking, molecular dynamics simulations, and design as a drug for anti-graves' disease. Journal of Molecular Structure, 1289, Pp. 135913.https://doi.org/10.1016/j.molstruc.2023.135913

Edache, E.I., Uzairu, A., Mamza, P.A.P., and Shallangwa, G.A., 2020. Prediction of HemO Inhibitors Based on Iminoguanidine using QSAR, 3DQSAR Study, Molecular Docking, Molecular Dynamic Simulation, and ADMET. Journal of Drug Design and Discovery Research, 1 (2), Pp. 36-52.

Eldehna, W.M., Almahli, H., Ibrahim, T.M., Fares, M., Al-Warhi, T., Boeckler, F.M., Bekhit, A.A. and Abdel-Aziz, H.A., 2019. Synthesis, in vitro biological evaluation and in silico studies of certain arylnicotinic acids conjugated with aryl (thio) semicarbazides as a novel class of anti-leishmanial agents. European Journal of Medicinal Chemistry, 179, Pp. 335-346. https://doi.org/10.1016/j.ejmech.2019.06.051

Elfiky, A.A., Mahran, H.A., Ibrahim, I.M., Ibrahim, M.N. and Elshemey, W.M., 2022. Molecular dynamics simulations and MM-GBSA reveal novel guanosine derivatives against SARS-CoV-2 RNA dependent RNA polymerase. RSC advances, 12 (5), Pp. 2741-2750.

Eltayb, W.A., Abdalla, M., and Rabie, A.M., 2023. Novel investigational anti-SARS-CoV-2 agent ensitrelvir "S-217622": a very promising potential universal broad-spectrum antiviral at the therapeutic frontline of coronavirus species. ACS omega, 8 (6), Pp. 5234-5246. https://doi.org/10.1021/acsomega.2c03881

Fan, Y., Lu, Y., Chen, X., Tekwani, B., Li, X.C. and Shen, Y., 2018. Anti-Leishmanial and cytotoxic activities of a series of maleimides: synthesis, biological evaluation and structure-activity relationship. Molecules, 23 (11), Pp. 2878.https://doi.org/10.3390/molecules23112878

French, J.B., Yates, P.A., Soysa, D.R., Boitz, J.M., Carter, N.S., Chang, B., Ullman, B. and Ealick, S.E., 2011. The Leishmania donovani UMP synthase is essential for promastigote viability and has an unusual tetrameric structure that exhibits substrate-controlled oligomerization. Journal of Biological Chemistry, 286 (23), Pp. 20930-20941.https://doi.org/10.1074/jbc.M111.228213

Fuhrmann, J., Rurainski, A., Lenhof, H.P., and Neumann, D., 2010. A new Lamarckian genetic algorithm for flexible ligand-receptor docking. Journal of computational chemistry, 31 (9), Pp. 1911-1918.

Gandin, V., Khalkar, P., Braude, J., and Fernandes, A.P., 2018. Organic selenium compounds as potential chemotherapeutic agents for improved cancer treatment. Free Radical Biology and Medicine, 127, Pp. 80-97. https://doi.org/10.1016/j.freeradbiomed.2018.05.001

Gatreddi, S., Pillalamarri, V., Vasudevan, D., Addlagatta, A. and Qureshi, I.A., 2019. Unraveling structural insights of ribokinase from Leishmania donovani. International journal of biological macromolecules, 136, Pp. 253-265.https://doi.org/10.1016/j.ijbiomac.2019.06.001

Ghorbani, M. and Farhoudi, R., 2017. Leishmaniasis in humans: drug or vaccine therapy?. Drug design, development and therapy, pp.25-40. https://doi.org/10.2147/DDDT.S146521

Ibrahim, M.T., Uzairu, A., Uba, S., and Shallangwa, G.A., 2021. Design of more potent quinazoline derivatives as EGFR WT inhibitors for the treatment of NSCLC: a computational approach. Future Journal of Pharmaceutical Sciences, 7, Pp. 1-11.https://doi.org/10.1186/s43094-021-00279-3

Imberty, A., Hardman, K.D., Carver, J.P. and Perez, S., 1991. Molecular modelling of protein-carbohydrate interactions. Docking of monosaccharides in the binding site of concanavalin A. Glycobiology, 1 (6), Pp. 631-642.https://doi.org/10.1093/glycob/1.6.631

Jawarkar, R.D., Sharma, P., Jain, N., Gandhi, A., Mukerjee, N., Al-Mutairi, A.A., Zaki, M.E., Al-Hussain, S.A., Samad, A., Masand, V.H. and Ghosh, A., 2022. QSAR, molecular docking, MD simulation and MMGBSA calculations approaches to recognize concealed pharmacophoric features requisite for the optimization of ALK tyrosine kinase inhibitors as anticancer leads. Molecules, 27 (15), Pp. 4951.

Jerzy, K., 2003. Synthesis of new N-substituted cyclic imides with potential anxiolytic activity. XXV. derivatives of halogenodibenzo (eh) bicyclo (2.2. 2) otcane-2, 3-dicarboximide. Acta Pol Pharm., 60, Pp. 1183-1189.

Jorgensen, W.L. and Thomas, L.L., 2008. Perspective on free-energy perturbation calculations for chemical equilibria. Journal of chemical theory and computation, 4 (6), Pp. 869-876. https://doi.org/10.1021/ct800011m

Keurulainen, L., Siiskonen, A., Nasereddin, A., Kopelyanskiy, D., Sacerdoti-Sierra, N., Leino, T.O., Tammela, P., Yli-Kauhaluoma, J., Jaffe, C.L. and Kiuru, P., 2015. Synthesis and biological evaluation of 2-arylbenzimidazoles targeting Leishmania donovani. Bioorganic & Medicinal Chemistry Letters, 25 (9), Pp. 1933-1937.

Khan, M.I., Baloch, M.K. and Ashfaq, M., 2004. Biological aspects of new organotin (IV) compounds of 3-maleimidopropionic acid. Journal of organometallic chemistry, 689 (21), Pp. 3370-3378.

Kumar, V., Sharma, M., Rakesh, B.R., Malik, C.K., Neelagiri, S., Neerupudi, K.B., Garg, P. and Singh, S., 2018. Pyridoxal kinase: a vitamin B6 salvage pathway enzyme from Leishmania donovani. International journal of biological macromolecules, 119, Pp. 320-334. https://doi.org/10.1016/j.ijbiomac.2018.07.095

Landgraf, A.D., Alsegiani, A.S., Alaqel, S., Thanna, S., Shah, Z.A., and Sucheck, S.J., 2020. Neuroprotective and anti-neuroinflammatory properties of ebselen derivatives and their potential to inhibit neurodegeneration. ACS chemical neuroscience, 11 (19), Pp. 3008-3016.https://doi.org/10.1021/acschemneuro.0c00328.

Lawal, H.A., Uzairu, A. and Uba, S., 2021. QSAR, molecular docking studies, ligand-based design and pharmacokinetic analysis on Maternal Embryonic Leucine Zipper Kinase (MELK) inhibitors as potential anti-triple-negative breast cancer (MDA-MB-231 cell line) drug compounds. Bulletin of the National Research Centre, 45, Pp. 1-20. https://doi.org/10.1186/s42269-021-00541-x

Lee, J., Cheng, X., Jo, S., MacKerell, A.D., Klauda, J.B. and Im, W., 2016. CHARMM-GUI input generator for NAMD, GROMACS, AMBER, OpenMM, and CHARMM/OpenMM simulations using the CHARMM36 additive force field. Biophysical journal, 110 (3), Pp. 641a.

Li, W., Fan, Y., Shen, Z., Chen, X., and Shen, Y., 2012. Antifungal activity of simple compounds with maleic anhydride or dimethylmaleimide structure against Botrytis cinerea. Journal of Pesticide Science, 37 (3), Pp. 247-251.

Li, Z., Wan, H., Shi, Y. and Ouyang, P., 2004. Personal experience with four kinds of chemical structure drawing software: review on ChemDraw, ChemWindow, ISIS/Draw, and ChemSketch. Journal of chemical information and computer sciences, 44 (5), Pp. 1886-1890. https://doi.org/10.1021/ci049794h

Lipinski, C.A., Lombardo, F., Dominy, B.W., and Feeney, P.J., 2012. Experimental and computational approaches to estimate solubility and permeability in drug discovery and development settings. Advanced drug delivery reviews, 64, Pp. 4-17. https://doi.org/10.1016/s0169-409x(00)00129-0.

López, S.N., Castelli, M.V., de Campos, F., Corrêa, R., Cechinel Filho, V., Yunes, R.A., Zamora, M.A., Enriz, R.D., Ribas, J.C., Furlán, R.L. and Zacchino, S.A., 2005. In vitro antifungal properties, structure-activity relationships and studies on the mode of action of N-phenyl, N-aryl, N-phenylalkyl maleimides and related compounds. Arzneimittelforschung, 55 (02), Pp. 123-132.

Mamgain, R., Kostic, M. and Singh, F.V., 2023. Synthesis and antioxidant properties of organoselenium compounds. Current medicinal chemistry, 30 (21), Pp. 2421-2448.https://doi.org/10.2174/0929867329666220801165849

Massova, I., and Kollman, P.A., 2000. Combined molecular mechanical and continuum solvent approach (MM-PBSA/GBSA) to predict ligand binding. Perspectives in drug discovery and design, 18, Pp. 113-135.

Muniba, F., 2019. Tutorial: molecular dynamics (MD) simulation using Gromacs. Bioinformatics Review, 5, Pp. 12.

Nipun, T.S., Khatib, A., Ibrahim, Z., Ahmed, Q.U., Redzwan, I.E., Primaharinastiti, R., Saiman, M.Z., Fairuza, R., Widyaningsih, T.D., AlAjmi, M.F. and Khalifa, S.A., 2021. GC-MS-and NMR-based metabolomics and molecular docking reveal the potential alpha-glucosidase inhibitors from psychotria malayana jack leaves. Pharmaceuticals, 14 (10), Pp. 978.

Nishiguchi, T., Yoshikawa, Y., and Yasui, H., 2017. Anti-diabetic effect of organo-chalcogen (sulfur and selenium) Zinc complexes with hydroxy-pyrone derivatives on leptin-deficient Type 2 diabetes model ob/ob mice. International Journal of Molecular Sciences, 18 (12), Pp. 2647.

Ou-Yang, S.S., Lu, J.Y., Kong, X.Q., Liang, Z.J., Luo, C. and Jiang, H., 2012. Computational drug discovery. Acta Pharmacologica Sinica, 33 (9), Pp. 1131-1140.https://doi.org/10.1038/aps.2012.109

Pathak, R.K., Singh, D.B., Sagar, M., Baunthiyal, M., and Kumar, A., 2020. Computational approaches in drug discovery and design. Computer-aided drug design, Pp. 1-21.

Patle, S.K., Kawathekar, N., Zaveri, M. and Kamaria, P., 2013. Synthesis and evaluation of 2, 4, 6-trisubstituted pyrimidine derivatives as novel antileishmanial agents. Medicinal Chemistry Research, 22 (4), Pp. 1756-1761.

Pires, D.E., Blundell, T.L., and Ascher, D.B., 2015. pkCSM: predicting small-molecule pharmacokinetic and toxicity properties using graph-based signatures. Journal of medicinal chemistry, 58 (9), Pp. 4066-4072. https://doi.org/10.1021/acs.jmedchem.5b00104.

Quintão, N.L., da Silva, G.F., Antonialli, C.S., de Campos-Buzzi, F., Corrêa, R., and Cechinel Filho, V., 2010. N-antipyrine-3, 4-dichloromaleimide, an effective cyclic imide for the treatment of chronic pain: the role of the glutamatergic system. Anesthesia & Analgesia, 110 (3), Pp. 942-950.

Radomska, D., Czarnomysy, R., Radomski, D. and Bielawski, K., 2021. Selenium compounds as novel potential anticancer agents. International Journal of Molecular Sciences, 22 (3), Pp. 1009. https://doi.org/10.3390/ijms22031009

Raj, I., Kumar, S. and Gourinath, S., 2012. The narrow active-site cleft of O-acetylserine sulfhydrylase from Leishmania donovani allows complex formation with serine acetyltransferases with a range of C-terminal sequences. Acta Crystallographica Section D: Biological Crystallography, 68 (8), Pp. 909-919. https://doi.org/10.1107/S0907444912016459

Sahakyan, H., 2021. Improving virtual screening results with MM/GBSA and MM/PBSA rescoring. Journal of Computer-Aided Molecular Design, 35 (6), Pp. 731-736. https://doi.org/10.1007/s10822-021-00389-3

Shaukat, A., Mirza, H.M., Ansari, A.H., Yasinzai, M., Zaidi, S.Z., Dilshad, S. and Ansari, F.L., 2013. Benzimidazole derivatives: synthesis, leishmanicidal effectiveness, and molecular docking studies. Medicinal Chemistry Research, 22, Pp. 3606-3620.

Shen, Z., Fan, Y., Li, F., Chen, X. and Shen, Y., 2013. Synthesis of N-substituted dimethylmaleimides and their antifungal activities against Sclerotinia sclerotiorum. Journal of pest science, 86, Pp. 353-360.

Slavica, A., Dib, I. and Nidetzky, B., 2007. Selective modification of surface-exposed thiol groups in Trigonopsis variabilisd-amino acid oxidase using poly (ethylene glycol) maleimide and its effect on activity and stability of the enzyme. Biotechnology and bioengineering, 96 (1), Pp. 9-17.

Soufari, H., Waltz, F., Parrot, C., Durrieu-Gaillard, S., Bochler, A., Kuhn, L.,

Sissler, M. and Hashem, Y., 2020. Structure of the mature kinetoplastids mitoribosome and insights into its large subunit biogenesis. Proceedings of the National Academy of Sciences, 117 (47), Pp. 29851-29861. https://doi.org/10.1073/pnas.2011301117

Stevanovic, S., Sencanski, M., Danel, M., Menendez, C., Belguedj, R., Bouraiou, A., Nikolic, K., Cojean, S., Loiseau, P.M., Glisic, S. and Baltas, M., 2019. Synthesis, in silico, and in vitro evaluation of anti-leishmanial activity of oxadiazoles and indolizine containing compounds flagged against anti-targets. Molecules, 24 (7), Pp. 1282. https://doi.org/10.3390/molecules24071282

Straatsma, T.P. and Berendsen, H.J.C., 1988. Free energy of ionic hydration: Analysis of a thermodynamic integration technique to evaluate free energy differences by molecular dynamics simulations. The Journal of chemical physics, 89 (9), Pp. 5876-5886.

Torres-Gómez, H., Hernández-Núñez, E., León-Rivera, I., Guerrero-Alvarez, J., Cedillo-Rivera, R., Moo-Puc, R., Argotte-Ramos, R., del Carmen Rodríguez-Gutiérrez, M., Chan-Bacab, M.J. and Navarrete-Vázquez, G., 2008. Design, synthesis and in vitro antiprotozoal activity of benzimidazole-pentamidine hybrids. Bioorganic and medicinal chemistry letters, 18 (11), Pp. 3147-3151.

Ugbe, F.A., Edache, E.I., Adeniji, S.E., Arthur, D.E., Ajala, A., Adawara, S.N., Ejeh, S., and Ibrahim, Z.Y.U., 2024. Computational evaluation of the inhibitory potential of some urea, thiourea, and selenourea derivatives of diselenides against leishmaniasis: 2D-QSAR, pharmacokinetics, molecular docking, and molecular dynamics simulation. Journal of Molecular Structure, 1302, Pp. 137473. https://doi.org/10.1016/j.molstruc.2023.137473.

Ugbe, F.A., Shallangwa, G.A., and Adamu Uzairu, I.A., 2023b. Combined QSAR modeling, molecular docking screening, and pharmacokinetics analyses for the design of novel 2, 6-diarylidene cyclohexanone analogs as potent anti-leishmanial agents. Progress in Chemical and Biochemical Research, 6 (1), Pp. 11-30.

Ugbe, F.A., Shallangwa, G.A., Uzairu, A. and Abdulkadir, I., 2021. Activity modeling, molecular docking and pharmacokinetic studies of some boron-pleuromutilins as anti-wolbachia agents with potential for treatment of filarial diseases. Chemical Data Collections, 36, Pp.100783. https://doi.org/10.1016/j.cdc.2021.100783.

Ugbe, F.A., Shallangwa, G.A., Uzairu, A. and Abdulkadir, I., 2022a. Theoretical activity prediction, structure-based design, molecular docking and pharmacokinetic studies of some maleimides against Leishmania donovani for the treatment of leishmaniasis. Bulletin of the National Research Centre, 46 (1), Pp. 92. https://doi.org/10.1186/s42269-022-00779-z

Ugbe, F.A., Shallangwa, G.A., Uzairu, A. and Abdulkadir, I., 2022b. A combined 2-D and 3-D QSAR modeling, molecular docking study, design, and pharmacokinetic profiling of some arylimidamide-azole hybrids as superior L. donovani inhibitors. Bulletin of the National Research Centre, 46 (1), Pp. 189. https://doi.org/10.1186/s42269-022-00874-1

Ugbe, F.A., Shallangwa, G.A., Uzairu, A. and Abdulkadir, I., 2022d. Molecular Docking Screening and Pharmacokinetic Studies of Some Boron-Pleuromutilin Analogues against Possible Targets of Wolbachia pipientis. Journal of Molecular Docking, 2 (1), Pp. 29-43. https://doi.org/10.33084/jmd.v2i1.3450

Ugbe, F.A., Shallangwa, G.A., Uzairu, A. and Abdulkadir, I., 2023a. A 2-D QSAR modeling, molecular docking study and design of 2-Arylbenzimidazole derivatives as novel leishmanial inhibitors: a molecular dynamics study. Advan J Chem Sect A, 6 (1), Pp. 50-64. DOI: 10.22034/pcbr.2022.366493.123.

Ugbe, F.A., Shallangwa, G.A., Uzairu, A. and Abdulkadir, I., 2023d. Molecular docking investigation, pharmacokinetic analysis, and molecular dynamic simulation of some benzoxaborole-benzimidazole hybrids: An approach to identifying superior onchocerca inhibitors. Borneo Journal of Pharmacy, 6 (1), Pp. 58-78. doi:10.33084/bjop.v6i1.3876

Ugbe, F.A., Shallangwa, G.A., Uzairu, A., Abdulkadir, I., Edache, E.I., Al-Megrin, W.A.I., Al-Shouli, S.T., Wang, Y. and Abdalla, M., 2023c. Cheminformatics-based discovery of new organoselenium compounds with potential for the treatment of cutaneous and visceral leishmaniasis. Journal of Biomolecular Structure and Dynamics, Pp. 1-24. https://doi.org/10.1080/07391102.2023.2279269.

Ugbe, F.A., Shallangwa, G.A., Uzairu, A., and Abdulkadir, I., 2022c. Molecular docking-based virtual screening, molecular dynamic simulation, and 3-D QSAR modeling of some pyrazolopyrimidine analogs as potent anti-filarial agents. In Silico Pharmacology, 10 (1), Pp. 21. https://doi.org/10.1007/s40203-022-00136-y

Umar, A.B., and Uzairu, A., 2023. New flavone-based arylamides as potential V600E-BRAF inhibitors: Molecular docking, DFT, and pharmacokinetic properties. Journal of Taibah University Medical Sciences, 18 (5), Pp. 1000-1010.

Wang, X., Dong, H. and Qin, Q., 2020. QSAR models on aminopyrazole-substituted resorcylate compounds as Hsp90 inhibitors. J Comput Sci Eng, 48, Pp. 1146-1156. http://www.asocse.org

Zamzami, M.A., 2023. Molecular docking, molecular dynamics simulation and MM-GBSA studies of the activity of glycyrrhizin relevant substructures on SARS-CoV-2 RNA-dependent-RNA polymerase. Journal of Biomolecular Structure and Dynamics, 41 (5), Pp. 1846-1858.